

## Derivation of the low-energy optical-absorption spectra of *a*-Si:H from photoconductivity

G. Moddel, D. A. Anderson, and William Paul

*Gordon McKay Laboratory, Division of Applied Sciences, Harvard University, Cambridge, Massachusetts 02138*

(Received 3 March 1980)

We outline a procedure to extract the optical-absorption coefficient as a function of energy from measurements of photoconductivity and assess the assumptions involved in applying it to *a*-Si:H. Using this procedure, we obtain accurate absorption spectra in the range from 1.8 to below 1.2 eV. These spectra show an absorption shoulder around 1.3 eV which we analyze in terms of possible optical transitions involving specific distributions of states in the gap.

### I. INTRODUCTION

One of the important problems in the study of amorphous semiconductors is the determination of the density-of-states distribution in the pseudo-gap. The curve of absorption coefficient  $\alpha$  versus photon energy  $h\nu$  yields a joint valence-band-conduction-band density of states, when one makes the usual assumption that the matrix element for absorption is independent of  $h\nu$ . However, the use of this technique to obtain information about states in the gap requires the measurement of low  $\alpha$ . In amorphous semiconductors such as *a*-Si:H alloys which are usually prepared as thin films of thickness on the order of 10  $\mu\text{m}$  or less, the thin film geometry limits the accurate determination of  $\alpha$  from optical transmission and reflection data to  $\alpha \gtrsim 10 \text{ cm}^{-1}$ .

Drawing on the work done on the use of photoconductivity  $\Delta\sigma$  in the detection of weak absorption involving impurity levels in crystalline semiconductors,<sup>1</sup> a number of authors have sought to make use of photoconductivity spectra to obtain information about sub-band-gap absorption in amorphous materials.<sup>2-7</sup> In general, however, the information is largely qualitative.

In this paper we outline a procedure, dependent upon a set of assumptions labeled (A) through (G), which can be used quantitatively to derive the relative optical-absorption coefficient from measurements of photoconductivity. We then assess the validity of each of these assumptions in the particular case of *a*-Si:H films from an examination of experimental results for the sputtered samples prepared in this laboratory. We conclude that one can with confidence obtain the relative-absorption coefficient from 1.8 to below 1.2 eV, and that the data confirm our earlier study<sup>8-10</sup> showing structure in the joint density of states in the region of 1.2 to 1.4 eV. The possible optical transitions giving rise to this structure and the implications for the distribution of gap states are also discussed.

### II. OUTLINE OF NORMALIZATION

Under the condition (A) that illumination and electron-hole generation are uniform throughout the material, the photoconductivity may be written as

$$\Delta\sigma = F\alpha\eta e\mu_D\tau_R, \quad (1)$$

where  $F$  is the incident photon flux per unit area,  $\alpha$  the absorption coefficient,  $\eta$  the quantum efficiency for photocarrier generation,  $\mu_D$  the drift mobility of the dominant photocarrier, and  $\tau_R$  the response time of photoconductivity.<sup>4</sup> It is assumed (B) that reflection at the front and back surfaces of the film and the resulting interference may be ignored. Expression (1) is also based on the assumption (C) that there is only one type of photocarrier (the electron) contributing to the photocurrent over the photon energy range of interest.

The intensity dependence of the photocurrent  $I_p$  may be expressed as

$$I_p \propto F^\beta, \quad (2)$$

where  $\beta$  is an empirical exponent. For different samples, we find that  $0.5 \leq \beta \leq 1$  for a given excitation energy  $h\nu$  and a given  $\alpha$ . To obtain  $\Delta\sigma(h\nu)$  independent of the variation of  $F$  with  $h\nu$ , the data may be normalized such that

$$\Delta\sigma(h\nu) \propto I_p(h\nu, F)(F_0/F)^\beta, \quad (3)$$

where  $F_0$  is a reference flux, usually  $10^{15}$  photons  $\text{cm}^{-2} \text{s}^{-1}$  in our work. Earlier published photoconductivity spectra from this laboratory<sup>5,8-10</sup> were normalized according to this relation.

To extract  $\alpha(h\nu)$  from photoconductivity data involves making further assumptions which will be justified in a later section of this paper. The dependence of  $I_p$  (and therefore also of  $\Delta\sigma$ ) on incident intensity, as expressed in relation (2), is an experimental observation. However,  $I_p$  must depend on the number of *absorbed* photons in the film, which is a function of both the *incident* photon flux and the absorption coefficient. The effect of

increasing  $\alpha$  should be identical to that of increasing  $F$  in creating additional photocarriers. Therefore we may generalize relation (2) so that

$$I_p \propto (\alpha F)^\beta. \quad (4)$$

This expression may be used to normalize the data as a function of photon energy provided (D) that conditions are chosen such that  $\beta$  does not vary with  $h\nu$ . We assume (*e, f, g*) that the remaining terms in Eq. (1),  $\tau_R$ ,  $\mu_D$ , and  $\eta$ , are independent of  $h\nu$  in the energy range of interest. From (4) we may then write

$$\frac{\alpha(h\nu)}{\alpha_0} = \frac{F_0 \left( \frac{I_p(h\nu, F)}{I_{p0}} \right)^{1/\beta}}{F}, \quad (5)$$

where the subscript 0 refers to some reference energy  $h\nu_0$ , and  $\alpha_0$  is the absorption coefficient at  $h\nu_0$ .

In summary, Eq. (5) may be viewed as a normalization of photoconductivity data to yield relative absorption spectra under the conditions that  $\eta\mu_D\tau_R$  does not vary with  $h\nu$ , and variations in  $\eta\mu_D\tau_R$  with  $F$  are compensated for by the normalization of Eqs. (4) and (5).

### III. EXPERIMENTAL METHODS

The photoconductivity was measured using two coplanar Nichrome electrodes evaporated onto *a*-Si:H films with a 200- $\mu$ m gap 2 mm in length. Current-voltage characteristics were linear in the dark and under illumination in the region of the applied fields, which ranged from 50 to 500 V/cm. Both zero frequency and ac photocurrents could be accurately determined down to  $10^{-13}$  A using a Keithley 602 electrometer in current mode and an Ithaco 393 lock-in analyzer with a current preamplifier, respectively. The radiation from a tungsten source, dispersed by a Leiss double-prism monochromator with slits selected to give better than 0.03-eV resolution, illuminated the sample which was mounted in an evacuated, temperature-controlled Janis optical cryostat. Except where noted, the measurements reported here were taken at room temperature. The illumination intensity was monitored by detecting the chopped radiation from a beam splitter on a calibrated thermopile. Independent photoconductivity measurements with known higher photon fluxes at 1.2 eV were made by using a Nd-YAG laser to illuminate the samples.

The samples used in this study are typical of those we have made by rf sputtering of Si onto Corning 7059 glass substrates in an argon-hydrogen atmosphere. Their thickness is on the order of 10  $\mu$ m. Further details concerning the deposition are published elsewhere.<sup>11</sup> None of the films

discussed here showed evidence of a change in the dark conductivity or photoconductivity after illumination.<sup>12</sup>

## IV. ANALYSIS OF ASSUMPTIONS

### A. Uniform illumination

The assumption of uniform electron-hole pair generation can be readily met by using a sample whose thickness  $t$  is such that the condition  $\alpha t \ll 1$  is satisfied for the range of excitation energies over which this technique is to be used. Since we are primarily interested in using this technique in an energy range where  $\alpha \leq 10^3$  cm<sup>-1</sup>, this condition can be easily satisfied for our sample thickness in the range 1 to 10  $\mu$ m.

### B. Reflection

Between 1.2 and 1.8 eV the total reflectance from a 10- $\mu$ m film varies from 25% to 30% (see Ref. 13). The correction which must be applied to  $F$  to account for the energy dependence of the reflectivity at front and back surfaces is therefore a small one, and is insignificant compared with other limits to the accuracy of the present technique. We emphasize that in this analysis we are not concerned with the absolute magnitude of the photoconductivity which would require a consideration of the magnitude of reflectivity. This is necessary, for example, if a comparison of photoconductivity and optical absorption is used to obtain the electron  $\mu_D\tau_R$  product. Instead, we seek only a photoconductivity-derived spectrum proportional to  $\alpha(h\nu)$ , which is then placed on an absolute scale by fitting it to the results from a direct transmission measurement. For this we require simply that the reflectivity does not vary with  $h\nu$ .

Interference fringes resulting from front and back surface reflections were not visible for the films studied here, because their spacing in the photoconductivity spectra is less than the resolution of the spectrometer used in the measurements. For thinner films it would be necessary to average through the fringes.

### C. Dominant electronic photoconduction

While identification of the dominant carrier in a photoconductivity experiment is rarely straightforward, it is easier to identify in a Schottky diode configuration. For those of our *a*-Si:H films which are photoconductive and show a significant photovoltaic effect, an analysis of the spectral dependence of the short circuit current<sup>14</sup> indicates that the  $\mu_D\tau_R$  product for holes is of the order of  $10^{-10}$  cm<sup>2</sup>/V, substantially lower than the value of

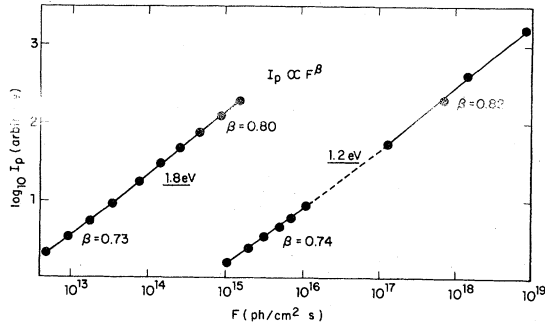


FIG. 1. Zero-frequency photocurrent  $I_p$ , plotted as a function of incident photon flux  $F$ , for 1.2- and 1.8-eV excitation. The slope  $\beta$  is indicated for high and low illumination levels. A tungsten source and monochromator supplied the illumination except for the high flux region of the 1.2-eV curve, where an Nd-YAG laser was used.

$10^{-6}$  cm<sup>2</sup>/V for electrons deduced from photoconductivity measurements at band-gap energies.<sup>15</sup> The fact that the conduction-band electron remains the dominant photocarrier for all  $h\nu$  of interest is a consequence of the arguments concerning  $\mu_D$  and  $\eta$  which follow.

#### D. Intensity dependence

In Fig. 1 we show the intensity dependence of the photocurrent of a typical sample at two different excitation energies. At each energy there is no single value of  $\beta$  which describes the data over the entire range of intensities used. However, we can define ranges of intensity or, more usefully, ranges of photocurrent, for which  $\beta$  is essentially constant. Note also that the two curves are virtually identical except for a translation along the abscissa; therefore, if we restrict our experimental conditions to keep the photocurrent within a given range,  $\beta$  is independent of excitation energy.<sup>16</sup>

#### E. Response time

The response time  $\tau_R$ , measured from the decay of the photocurrent after illumination, generally increases as  $h\nu$  is reduced below band-gap energies in  $a$ -Si:H samples for which  $\beta < 1$ . Increases in  $\tau_R$  by a factor of 50 when  $h\nu$  is reduced from 1.49 to 0.99 eV have been reported.<sup>8</sup> We examine below the origin of this apparent energy dependence of  $\tau_R$  by considering the sample whose photocurrent depends on intensity as shown in Fig. 1. The response time of the photocurrent can be obtained very simply from the output of the lock-in amplifier as a function of chopping frequency. For decay times of the order of the reciprocal of the chopping frequency, the lock-in

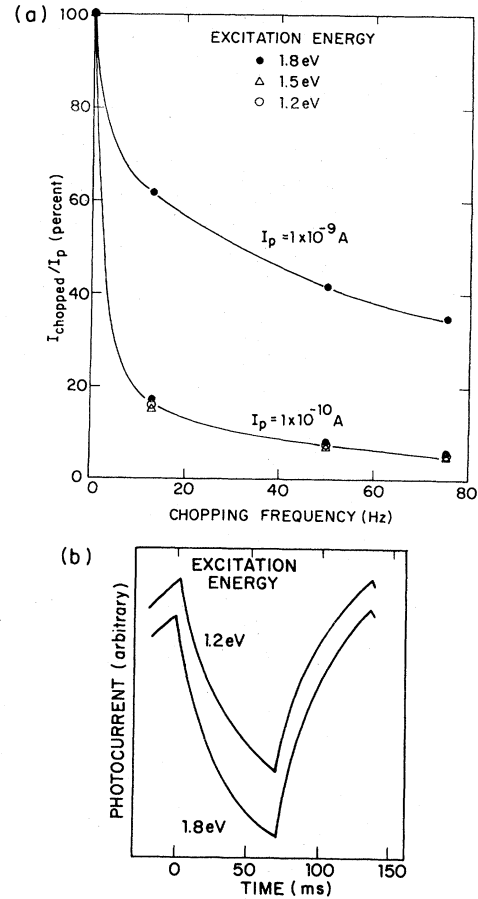


FIG. 2. (a) Ratio of chopped photocurrent to zero-frequency photocurrent  $I_p$ , plotted as a function of chopping frequency. Illumination levels were set to give the values of  $I_p$  indicated. The upper curve was obtained at 1.8 eV, and the lower curve at the three photon energies indicated. (b) Photocurrent versus time under chopped illumination (7.7 Hz) plotted for two photon energies. The flux was adjusted to give equal zero-frequency photocurrents and the curves were obtained using a boxcar integrator with a 2-ms gate.

output will be attenuated. In Fig. 2(a) we plot the magnitude of the chopped photocurrent divided by the steady-state photocurrent, as a function of chopping frequency, for various conditions of illumination intensity and excitation energy.<sup>17</sup> In the upper curve we used an excitation energy of 1.8 eV, and the photon flux was adjusted to give a steady-state photocurrent  $I_p = 1 \times 10^{-9}$  A. The lower curve shows three sets of data using excitation energies of 1.8, 1.5, and 1.2 eV, and in each case the incident photon flux was adjusted to give a steady-state photocurrent  $I_p = 1 \times 10^{-10}$  A.

In both curves, as expected, there is a rapid reduction in the chopped signal with increasing chopping frequency between 0 and 75 Hz. The

greater reduction in the lower curve indicates that the response time is significantly longer than it is for the upper curve. The data of this figure demonstrate that  $\tau_R$  increases as the density of photocarriers in the material decreases, but there is no dependence of  $\tau_R$  on  $h\nu$  provided that  $I_p$  is kept constant with  $h\nu$ . Figure 2(b) shows this directly. Here we plot the time response of the photocurrent at energies of 1.2 and 1.8 eV, when the incident light intensity was adjusted for equal steady state  $I_p$ . The two curves, displaced vertically for clarity, are almost identical.

From these data we may infer that, at least between 1.2 and 1.8 eV,  $\tau_R$  depends not on the excitation energy as such but on the density of photocarriers in the material. The two, however, are easily confused because, for a given incident (rather than absorbed) flux, the weak absorption at lower  $h\nu$  creates fewer photocarriers.

The dependence of  $\tau_R$  on photocarrier density can be justified on physical grounds by considering that included in  $\tau_R$  is the effect of capture and release from shallow traps as well as recombination via capture by deep traps or directly with trapped holes. It is reasonable to suppose that the action of the deep states in the recombination process is a function of the occupation of all the states, which is, in turn, a function of electron-hole pair generation in the samples, and this leads quite naturally to the observed sublinear dependence of the photocurrent on light intensity. We comment on the consequences of the lack of dependence of  $\tau_R$  on  $h\nu$  in the Discussion section.

#### F. Drift mobility

It was deduced above (C) that the electron is the dominant photocarrier at high  $h\nu$ . We now consider whether it remains so and has a constant  $\mu_D$  over the photon energy range of interest. First we assume this to be correct and plot  $\alpha/\alpha_0$ , as expressed in Eq. (5), for photoconductivity data obtained at two temperatures in a typical undoped sample. In view of the continuous distribution of states which extends from the band edge into the gap, Eq. (1) has been written in terms of trap controlled transport ( $\mu_D$ ) and recombination ( $\tau_R$ ). The temperature dependence of  $\mu_D$  will show activated behavior with an activation energy which reflects the energy range of the trapping states below the band.<sup>4</sup> Therefore, if the drift mobility changed with excitation energy, either because of a shift in the transport level or because of a variation in the range of trapping states, we would expect the derived  $\alpha/\alpha_0$  curves to show a strong temperature dependence.

For temperatures of  $-107$  and  $60^\circ\text{C}$ , application

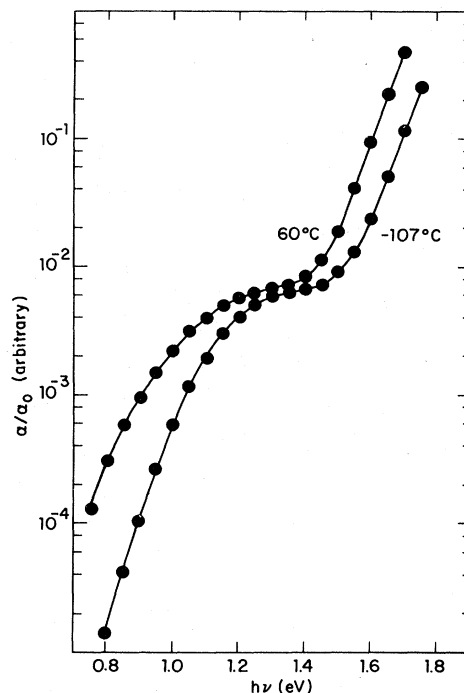


FIG. 3. Relative absorption coefficient  $\alpha/\alpha_0$ , deduced using Eq. (5), plotted as a function of photon energy  $h\nu$  for data obtained at two temperatures.

of Eq. (5) yields the two curves of  $\alpha/\alpha_0$  versus  $h\nu$  shown in Fig. 3. Within our 20% experimental error the curves are identical in shape above 1.2 eV. The horizontal displacement of  $6 \times 10^{-4}$  eV/K is not inconsistent with the observed temperature dependence of the absorption edge.<sup>18,19</sup> Below 1.0 eV the curves appear to diverge, indicating that the phototransport may be changing here. However, the measured photocurrent in this energy region fell below that for which  $\beta$  was determined to be constant. Because the  $\alpha/\alpha_0$  curves translate rigidly above 1.2 eV, we conclude that our assumptions of dominant electron photoconductivity in the conduction band, with constant  $\mu_D$ , are valid in this excitation region.

#### G. Quantum efficiency

A reduced quantum efficiency may result from any absorption process in a sample of  $a\text{-Si:H}$  which does not produce an electron at or near the conduction-band edge. Only electrons which are excited to states from which they can maintain a quasi-thermal-equilibrium with the band contribute to photoconductivity. Note that it is not necessary that every photocarrier be conducting for its entire lifetime, merely that many trapping and release cycles can occur before the carriers recombine. We discuss here two mechanisms which

might result in a lowering of  $\eta$ .

First, at low temperatures geminate excitons are formed which recombine radiatively and give photoluminescence before they can contribute to photoconduction. This would seriously reduce the quantum efficiency of the photoconductivity at low temperatures, but as the temperature is raised, the excitons dissociate thermally so that by room temperature there is no observable luminescence.<sup>20</sup> We must conclude that the great majority of the carriers at room temperature contribute to photoconduction and that this effect on  $\eta$  is small.

Second, any absorption into localized states which cannot maintain thermal equilibrium with the band will not contribute to photoconduction. Given the low density of states in the gap, this will effect  $\eta$  very little at energies corresponding to band-to-band transitions; however, its effect may increase as the excitation energy is reduced, giving rise to a strong energy dependence of  $\eta$ . The effect on our derived curve, in which we assume constant  $\eta$ , would be to reduce the derived  $\alpha$  at lower energies to less than its true value. Until we have more information we must, therefore, regard plots of  $\alpha$  derived from photoconductivity data as lower limits to  $\alpha$ , particularly at low  $h\nu$ .

## V. DISCUSSION

### A. Low energy optical absorption

In Fig. 4 we plot  $\alpha(h\nu)$  obtained from transmission measurements for a 10- $\mu\text{m}$ -thick sputtered  $a\text{-Si:H}$  film. Below 1.5 eV the errors in the reduction of the data lead to very large errors in  $\alpha$ . We now make use of the photoconductivity results to extend the range of energy by evaluating  $\alpha/\alpha_0$  using Eq. (5) and then fitting the result to the absolute absorption scale at one energy where the two sets of data overlap. In the figure this fit has been made at 1.6 eV, but the match between the two curves is so good in the region of overlap that it might have been made at any energy between 1.5 and 1.7 eV.

Using a thick film to demonstrate this technique, we can obtain direct absorption measurements to energies closer to 1.2 eV, which is the region in which we are particularly interested. The energy range of overlap cannot be extended by the choice of a different film thickness, merely shifted in energy. The upper limit is determined by the condition that  $\alpha t \ll 1$  which, for the data of Fig. 4, breaks down above 1.7 eV ( $\alpha = 10^3 \text{ cm}^{-1}$ ). The lower limit is set by the approximate condition  $\alpha t \geq 0.05$  in order that the absorption can be obtained from transmission data with reasonable

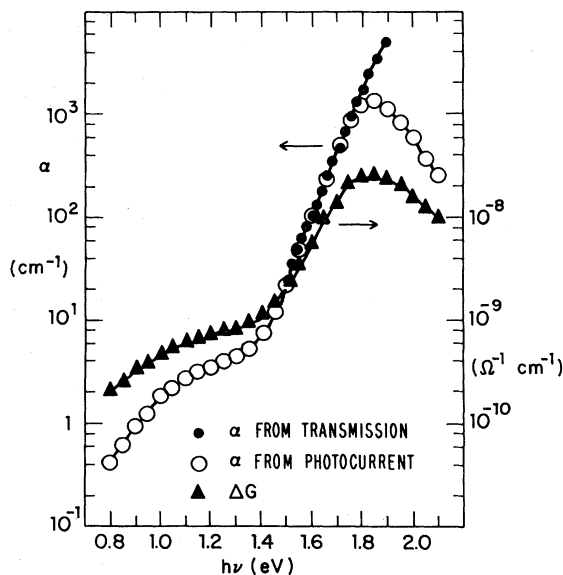


FIG. 4. ●●● Absorption coefficient  $\alpha$  versus photon energy  $h\nu$  for a typical 10- $\mu\text{m}$ -thick film from transmission measurements; ○○○ relative absorption  $\alpha/\alpha_0$  for the same sample using photoconductivity data in Eq. (5) and fitting to absolute  $\alpha$  curve at 1.6 eV. ▲▲▲ The same photoconductivity data normalized using Eq. (3) to give the photoconductive response  $\Delta G$ .

accuracy.

For the reasons discussed above, we believe that the only significant energy dependence in the photoconductivity-derived curves comes from the spectral dependence of  $\alpha$  in the range from 1.2 to 1.8 eV. Below 1.5 eV the photoconductivity data show a clear shoulder which we believe to be a genuine effect in the absorption.

To demonstrate the importance of the proper normalization of the data with respect to  $\beta$ , we also plot in Fig. 4 the spectral dependence of the zero-frequency photoconductive response<sup>21</sup>  $\Delta G$ , normalized to  $10^{15}$  photons  $\text{cm}^{-2} \text{ s}^{-1}$  using relation (3). In contrast to the  $\alpha(h\nu)$  derived from photoconductivity, the slope of this curve is significantly different from that of the  $\alpha(h\nu)$  derived from transmission measurements in the energy range of overlap. This sensitivity to the exact method of normalization gives us additional confidence in the  $\alpha(h\nu)$  derived from photoconductivity by the present procedure.

Although we have demonstrated the plausibility of the shoulder at 1.2 eV seen in photoconductivity spectra being a genuine shoulder in the absorption, final confirmation of this result must await a reliable direct measurement of  $\alpha$  down to values  $\sim 1 \text{ cm}^{-1}$  for undoped films of  $a\text{-Si:H}$ . However, when these films are phosphorus-doped, the 1.2-eV feature in the photoconductivity spectrum be-

comes much more pronounced.<sup>9,22</sup> The corresponding  $\alpha$  becomes large enough to be observed in transmission measurements.<sup>23</sup> This correlation enhances the credibility of the features seen in  $\alpha/\alpha_0$  at lower energies in the undoped films.

To make connection with our earlier publications,<sup>5,8-10</sup> we mention in passing that photoconductivity spectra, determined from measurements under illumination chopped at 13 Hz and normalized using relation (3), appear very similar to  $\alpha/\alpha_0$  curves from zero frequency measurements using Eq. (5). The reason is that, as  $h\nu$  decreases,  $\alpha$  decreases and  $\tau_R$  (at constant  $F$ ) increases. As  $\tau_R$  increases, the output signal from the lock-in analyzer is attenuated, with the net result that the increase in  $\tau_R$ , which would augment the photocurrent, is approximately balanced by the attenuation of the lock-in.

#### B. The density-of-states distribution in the gap

The relative joint density of states of the material is given by  $\alpha(h\nu)$ , if the matrix elements for optical transitions are assumed independent of photon energy. We shall assume this is so over the limited range of  $h\nu$  considered here and thereby exclude the possibility of transitions between two localized states in the gap. We shall not try to estimate a matrix element, but shall concentrate on the relative joint density of states. Deduction of a relative single density of states in the energy gap generally requires the input of information from other types of measurement, but we can nevertheless restrict consideration of the transitions which explain the structure in  $\alpha(h\nu)$  to three broad classes: (i) excitation from states in the valence band to states in the gap which are sufficiently close to the conduction band to be in equilibrium with it, (ii) excitation from states near the Fermi level into levels deep in the conduction band followed by relaxation to the band edge, and (iii) excitation from states in the lower half of the gap directly into states in the conduction band close to the conduction level. These three transitions are shown schematically in Fig. 5. In the following three paragraphs we examine each of these transitions and find that, while there is no convincing evidence to reject any of them, we consider (iii) to fit the present data best.

(i) The extent of the energy range below the conduction-band edge over which a quasi-equilibrium is maintained can be estimated very approximately by considering the release rate for a carrier trapped at energy  $E_t$  below the band, given by

$$\tau_{\text{rel}}^{-1} \approx (N_c/N_t)\nu_{\text{ph}} \exp(-E_t/kT),$$

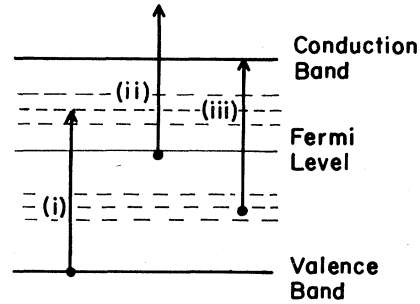


FIG. 5. Sub-band-gap transitions from (i) valence band to upper half of gap, (ii) below Fermi level to deep in conduction band, and (iii) lower half of gap to conduction-band edge.

where  $\nu_{\text{ph}}$  is a phonon frequency  $\sim 10^{13}$  Hz and  $N_c/N_t$  the ratio of the state densities in the band and trapping level. If  $\tau_{\text{rel}} > \tau_R$ , the trap controlled response time, then a carrier at that energy will have a greater probability for recombination than for excitation into the band. Only if  $\tau_{\text{rel}} \ll \tau_R$  will a quasi-equilibrium with the band be maintained. For our measured values of  $\tau_R$  in the range 1–100 ms and assuming  $N_c/N_t \sim 10^3$ , we find this latter condition can be satisfied for a depth of 0.7 eV below the band edge under our conditions of illumination. Valence-band to conduction-band transitions do not take place for  $h\nu \leq 1.8$  eV, so in the absence of a significant state density between the Fermi level and the valence-band edge, one might expect that transitions (i) could produce photocarriers only for  $h\nu \geq 1.1$  eV. Yet the shoulder in  $\alpha$  is seen to energies as low as 0.8 eV. Therefore, on the basis of this simple argument, transition (i) by itself appears an unlikely candidate to explain the spectra, although it could dominate for  $h\nu > 1.1$  eV.

(ii) We examine this possibility by considering a very crude model for the state distribution, calculating the relative joint density of states by integration, and then scaling to fit the experimental  $\alpha(h\nu)$ . As shown in Fig. 6(a), the density of states in the band away from the immediate vicinity of the band edge is assumed to vary as  $(E - E_0)^{1/2}$ , while in the gap we assume a constant density of states in the region immediately below the Fermi level. In this zero temperature model there is a threshold energy  $(E_0 - E_F)$  for optical absorption. In curve (a) of Fig. 7 we have fitted the experimental data of Fig. 4 using this model with  $E_0 - E_F$  as an adjustable parameter. The best fit to the data is obtained for  $E_0 - E_F = 0.71$  eV, which is not far from the measured conductivity activation energy  $E_g = 0.77$  eV. When applied to a larger number of samples, however, we find that this model fails in two respects: (1) the predicted on-

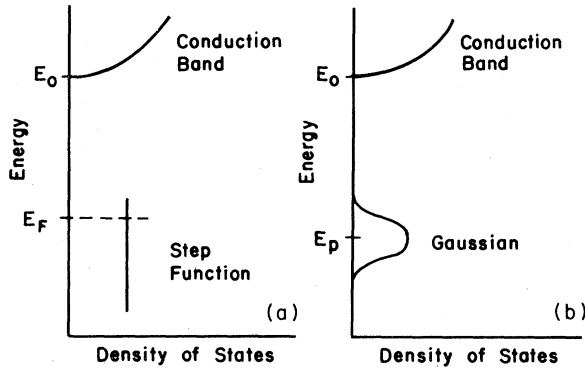


FIG. 6. Schematic model densities of states (DOS) used in fitting low energy  $\alpha(h\nu)$ . (a) Constant DOS at the Fermi level with a threshold for optical transitions at  $E_F$ . (b) A Gaussian distribution centered at  $E_p$  of FWHM  $E_w$  in an otherwise empty gap. In each case the DOS in the conduction band was assumed to be of the form  $N(E) \propto (E - E_0)^{1/2}$ .

set of photoconductivity or absorption is much sharper than that observed experimentally and (2) the threshold energy which fits the data best seems to vary little from sample to sample even in the case of phosphorus-doped material in which the Fermi level is shifted by several tenths of an eV. We must emphasize, however, that we have less confidence in our procedure for obtaining  $\alpha$  from  $\Delta\sigma$  at energies below 1.0 eV, and so cannot reject this class of transitions outright.

(iii) Curve (b) in Fig. 7 shows a similar fit to

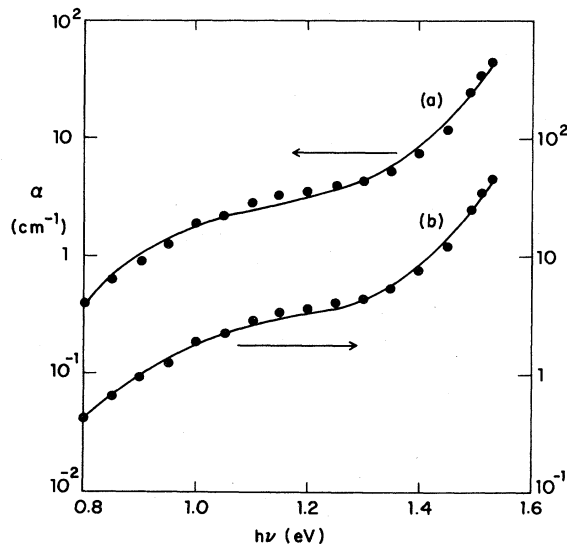


FIG. 7. Fit to experimental data points of Fig. 4 using the models of Fig. 6. Solid curve (a) was obtained assuming  $E_0 - E_F = 0.71$  eV, curve (b) by taking  $E_0 - E_p = 0.9$  eV and  $E_w = 0.35$  eV. Above 1.4 eV the data were fitted by adding the higher energy exponential dependence of  $\alpha$  on  $h\nu$  to the  $\alpha$  calculated from the models of Fig. 6.

the same experimental data using the model density of states shown in Fig. 6(b). Here we have assumed transitions are taking place from a Gaussian distribution of a given peak energy and given width into the same conduction band as before. The fit is slightly better than curve (a) in that it more accurately follows the overall shape of the shoulder. We do not, however, intend to imply that this is then an accurate model for the state density of this material. What is of significance is that the rising edge of the Gaussian distribution which best fits the data is very close to the threshold energy obtained from the best fit in (ii) above. Mathematically the sharp onset at the Fermi level is identical to a step function in  $g(E)$ , so both models give a best fit to the data which appears to predict a rapidly rising state density 0.7 to 0.8 eV below the energy level  $E_0$ . The position of  $E_0$  below the conduction level is not known accurately, but if we take it to be  $\sim 0.1-0.2$  eV, the approximate extent of the band tail, this places the onset of the feature in the state density about 1.0 eV below the conduction level. Since both models fit the data well in the photon energy range between 1.0 and 1.4 eV—a region in which we have confidence in the data—it is quite impossible to draw further conclusions about the shape of the state distribution deeper in the gap from  $\alpha(h\nu)$  alone. However, a correlation of photoemission and photoconductivity spectra appears to support our conclusion that situation (iii) is the most likely.<sup>24</sup>

We demonstrated earlier (Fig. 2) that  $\tau_R$  is not a function of  $h\nu$ ; therefore, we conclude that the recombination mechanism for the electron is independent of the energy at which the hole is created, at least between the valence-band edge and the suggested feature in the lower half of the gap. Evidently, the bottleneck to hole recombination is not between the valence-band edge and this feature, and it is likely that the state density remains high throughout the lower half of the gap.

## VI. CONCLUSIONS

It has been demonstrated that, within certain well-defined limitations, photoconductivity spectra can be used to obtain the absorption coefficient  $\alpha$  to energies lower than currently attainable by conventional techniques. We point out that, since the response time varies with the number of absorbed photons, the incident photon flux must be adjusted at each energy so that the intensity dependence of the zero-frequency photocurrent can be described by the same exponent. Under this condition, any photon energy dependence between 1.2 and 1.8 eV of the surface reflectivity, photoelectron drift mobility, quantum efficiency, and re-

sponse time can be neglected for  $a$ -Si:H in the reduction of the data. The photoconductivity data may then be normalized, using Eq. (5), to obtain relative absorption curves which show good agreement with results from optical transmission over the energy range of overlap, and are believed to yield accurate lower bounds to the absorption at least down to 1.2 eV.

These absorption curves show definite evidence of a shoulder in the region of 1.2 eV, which we believe to correspond to transitions from pseudo-gap states between the Fermi level and the valence-band edge into the conduction band. We are now applying this technique to study the effect of

preparation conditions on this shoulder and will present the results in a later publication.

#### ACKNOWLEDGMENTS

The authors wish to thank J. Blake for the optical-absorption measurements, and are grateful to R. W. Collins, P. Viktorovitch, and R. L. Weisfield for experimental and interpretive assistance, and to P. Ketchian for sample preparation. This work was supported by the National Science Foundation under Grants Nos. DMR-78-10014 and DMR-77-24295 and by the Joint Services Electronics Program under Contract No. N00014-75-C-0648.

<sup>1</sup>See, for example, Richard H. Bube, *Photoconductivity of Solids* (Wiley, New York, 1960), Chap. 6.

<sup>2</sup>J. E. Fischer and T. M. Donovan, *Opt. Commun.* **3**, 116 (1971).

<sup>3</sup>R. J. Loveland, W. E. Spear, and A. Al-Sharbaty, *J. Non-Cryst. Solids* **13**, 55 (1973/74).

<sup>4</sup>T. D. Moustakas and W. Paul, *Phys. Rev. B* **16**, 1564 (1977).

<sup>5</sup>T. D. Moustakas, D. A. Anderson, and William Paul, *Solid State Commun.* **23**, 155 (1977).

<sup>6</sup>Richard S. Crandall, *J. Non-Cryst. Solids* **35 & 36**, 381 (1980).

<sup>7</sup>J. I. Pankove, F. H. Pollak, and C. Schnabolk, *J. Non-Cryst. Solids* **35 & 36**, 459 (1980); G. D. Cody, B. Abeles, C. R. Wronski, B. Brooks, and W. A. Lanford, *ibid.*, **35 & 36**, 463 (1980).

<sup>8</sup>D. A. Anderson, G. Moddel, R. W. Collins, and W. Paul, *Solid State Commun.* **31**, 677 (1979).

<sup>9</sup>D. A. Anderson, G. Moddel, and W. Paul, *J. Non-Cryst. Solids* **35 & 36**, 345 (1980).

<sup>10</sup>R. W. Collins, M. A. Paesler, G. Moddel, and William Paul, *J. Non-Cryst. Solids* **35 & 36**, 681 (1980).

<sup>11</sup>D. A. Anderson, G. Moddel, M. A. Paesler, and William Paul, *J. Vac. Sci. Technol.* **16**, 906 (1979).

<sup>12</sup>Changes in the conductivity after exposure to light have been observed in  $a$ -Si:H by D. L. Staebler and C. R. Wronski, *Appl. Phys. Lett.* **31**, 292 (1977).

<sup>13</sup>E. C. Freeman (private communication).

<sup>14</sup>P. Viktorovitch (private communication). This is in agreement with the upper limit of  $\mu_D\tau_R$  for holes determined by D. L. Staebler, *J. Non-Cryst. Solids* **35 & 36**, 387 (1980).

<sup>15</sup>T. D. Moustakas, *J. Electron. Mater.* **8**, 391 (1979); and G. Moddel (unpublished).

<sup>16</sup>In some of the films we have studied, particularly those in which the Fermi level lies deeper in the gap ( $\sim 0.9$  eV from the conduction band), this is no longer true. Although  $\beta$  is a weak function of energy in these samples, the procedure we outline in this paper can still be used to obtain  $\alpha$  to good approximation.

<sup>17</sup>Quantitative analysis of the in-phase and quadrature components of the lock-in signal as a function of chopping frequency fail to yield self-consistent results, presumably because the rises and decays are not associated with a single exponential.

<sup>18</sup>Shifts of featureless edges can be difficult to interpret, since changes in the abscissa and ordinate may be indistinguishable. For Fig. 3 this is not a problem because the edge has a distinct feature and the horizontal and vertical shifts can be separately identified.

<sup>19</sup>E. C. Freeman and William Paul, *Phys. Rev. B* **20**, 716 (1979).

<sup>20</sup>M. A. Paesler and William Paul, *Philos. Mag.* (in press).

<sup>21</sup>Our photoconductive response  $\Delta G$  differs from photoconductivity  $\Delta\sigma$  in that no compensation has been made for nonuniform illumination throughout the bulk of the film. This is significant above 1.8 eV where  $\alpha$  is no longer much less than  $1/t$ .

<sup>22</sup>T. D. Moustakas (unpublished).

<sup>23</sup>J. C. Knights, in *Structure and Excitation of Amorphous Solids* (Williamsburg, Va., 1976), Proceedings of an International Conference on Structure and Excitation of Amorphous Solids, edited by G. Lucovsky and F. L. Galeener (Williamsburg, Va., 1976), p. 296; and independently observed in our laboratory.

<sup>24</sup>B. von Roedern and G. Moddel (unpublished).